

MODELING AND CONTROL BY INTEGRAL SLIDING MODE FOR GRID CONNECTED PHOTOVOLTAIC SYSTEM

A. BORNİ

Unité de Recherche Appliquée en Energies Renouvelables, URAER,
Centre de Développement des Energies Renouvelables, CDER, 47133 Ghardaïa, Algeria
Email : borni.abdelhalim@yahoo.fr

L. ZAROUR, R. CHENNI, & A. BOUZID

Laboratoire d'électrotechnique, Faculté des sciences de la technologie Université Constantine1. Algérie
Email : Laidzarour @hotmail.fr

Abstract: *This paper deals with a model of photovoltaic grid connected system using fourth order Runge-Kutta numerical method using MATLAB (m.file). The system configuration includes a photovoltaic generator, DC-DC converter, DC-AC inverter coupled to grid network. A robust maximum power point tracker (MPPT) using integral sliding mode controller is applied to the duty cycle value of the DC-DC converter which acts on power system. Mathematical modeling is developed and the simulation results confirm the validity of the proposed controller.*

Keywords: *Grid-connected photovoltaic system, Sliding mode controller, MPPT.*

1. Introduction

The world electricity demand is still increasing, which requires governments to set very effective policies to find new energy sources, more growth pressures of international unions for the protection of environment directs these countries to invest in clean energy (solar, wind ... etc.).

The tropical countries are based on the exploitation of solar energy because they contain a wide surface and the amount of the intensity of the sunlight can reach up to $1000\text{W} / \text{m}^2$. From this, the concept of our study is based on how to harvest the maximum of that energy for systems that are coupled to the grid. The optimization will be considered by the technique of sliding mode. of environment directs these countries to invest in clean energy (solar, wind ... etc.).

The tropical countries are based on the exploitation of solar energy because they contain a wide surface and the amount of the intensity of the sunlight can reach up to $1000\text{W} / \text{m}^2$. From this, the concept of our study is based on how to harvest the maximum of that energy for systems that are coupled to the grid. The optimization will be considered by the technique of sliding mode.

The typical configuration of the three-phase grid connected photovoltaic system is shown in Fig. 1. It consists of PV panel input capacitor C, Buck-Boost converter; three phases inverter and the grid. The Buck-Boost converter to adapt the load impedance to the photovoltaic generator; the three-phase inverter converts a DC input voltage into an AC sinusoidal voltage.

The controller has been proposed to overcome above problems. It consists of a MPPT controller and a voltage controller only. The MPPT controller by integral sliding mode technique generates the maximum power reference instead of duty cycle (D) of the Buck-Boost converter. The power reference generate the optimal quadratic current reference i_q^* , this last generates the quadratic voltage reference V_q^* . The second controller we assumed that the direct component current reference i_d^* is null, this current generating the direct voltage reference V_d^* . From this voltage and from the inverse Park transformation we obtain the three control voltages reference ($V_{sa}^*, V_{sb}^*, V_{sc}^*$).

The output power of PV panel is changed by irradiation and temperature. Since the characteristic curve of a PV panel exhibits a nonlinear I_{pv} - V_{pv} characteristic, a controller maximum power point tracker (MPPT) is required to match the PV panel power to the irradiation and temperature changes. Many algorithms have been developed for tracking maximum point of a PV panel such as perturb and observation, and incremental conductance (V. Salas et al., 2006), neural network (Yazdani et al., 2009) fuzzy logic control (Lalouni et al., 2009) and sliding mode controller (Song Kim ., 2006).

The sliding mode controller has robust control property under the presence of parameter variations and can achieve the tight regulation of the states for all operating point (Domingo et al., 2001; Mauro and Mario, 1996; Liang et al., 2001, Song Kim., 2006). In this study, an integral sliding mode controller applied to maximize the power of

photovoltaic generator has been proposed. The integral sliding mode controller can eliminate the steady state error by adding integral sliding surface, the choice of the sliding mode surface is expressed mathematically by: $(S(I_{pv}) = \partial P_{pv} / \partial I_{pv})$, while the output will be a change in the duty cycle of Buck-Boost converter.

To validate our study, the comparison of simulation results with those obtained by Song Kim [13], confirm what we obtained, under dynamic and permanent conditions.

Mathematical modeling is developed and simulation results verify the validity of the proposed controller.

2. Mathematical model of the grid system.

The grid connected system comprises a photovoltaic panel, a DC-AC inverter and a DC-DC converter to control the operation point of the PV panels and a sliding mode controller (Fig.1).

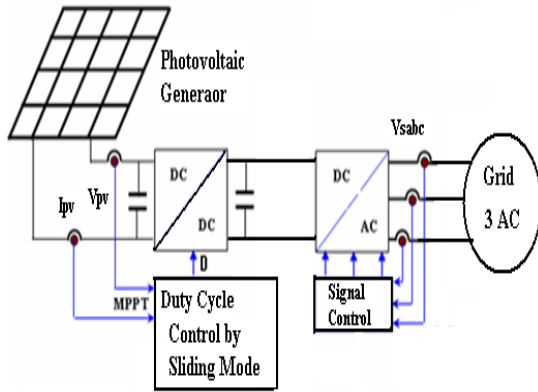


Fig.1. Schematic of the conversion chain

2.1. Photovoltaic generator model

An accurate equivalent circuit for the PV cell is shown in Fig.2 and Fig.3, the output current from the photovoltaic generator is given by equation (1) Appelbaum [9], Chenni [15].

$$I_{pv} = I_L - I_0 \left[\exp \left(\frac{q(V_{pv} + R_s I_{pv})}{\gamma K T_c} \right) - 1 \right] \quad (1)$$

The panel's parameters, changing with solar irradiance G (W/m^2) and temperature T ($^{\circ}K$), can be estimated by the following relations Appelbaum [9]:

$$\begin{cases} I_L = \left(\frac{G}{G_{ref}} \right) \left(I_{L,ref} + \mu_{Isc} (T_c - T_{c,ref}) \right) \\ I_0 = I_{0,ref} \left(\frac{T_c}{T_{c,ref}} \right)^3 \exp \left[\left(\frac{q \epsilon_G}{K A} \right) \left(\frac{1}{T_{c,ref}} - \frac{1}{T_c} \right) \right] \\ \gamma = \gamma_{ref} \left(\frac{T_{c,ref}}{T_c} \right) \end{cases} \quad (2)$$

Where I_{pv} and V_{pv} are the cell output current and voltage, and the definitions of the parameters are given in nomenclature.

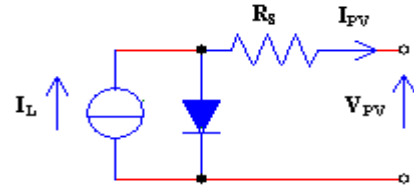


Fig.2. model represents solar cell circuit

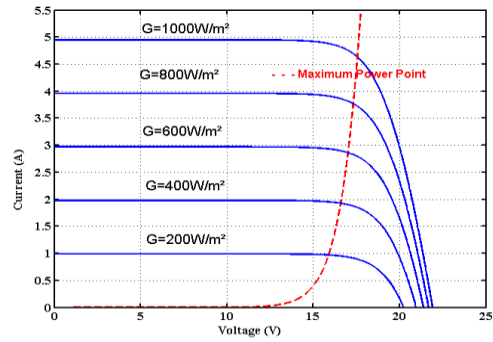


Fig.3. I_{pv} - V_{pv} Characteristics of PV panel at $T=25^{\circ}C$.

2.2. Solar subsystem

The dynamic model of the solar subsystem written in terms of voltage and current between input and output of the buck-boost converter can be expressed as: Valenciaga [6].

$$\begin{cases} \frac{dV_{pv}}{dt} = \frac{I_{pv}}{C} - \frac{i_L}{C} D \\ \frac{di_L}{dt} = \frac{V_{pv}}{L} D - \frac{V_s}{L} (1 - D) \\ \frac{dV_s}{dt} = \frac{i_L}{C} (1 - D) - \frac{i_s}{C} \end{cases} \quad (3)$$

Where i_s is the current injected on the DC-AC converter, L , C are electrical parameters of the DC-DC converter, D is the duty cycle.

2.3. Model of three phase grid

connected photovoltaic system

The state-space model of a three-phase grid-connected photovoltaic system shown in Fig. 1 can be described as follows [7].

$$\begin{cases} \frac{di_{sa}}{dt} = -\frac{R}{L}i_{sa} - \frac{R}{L}e_a + \frac{V_{sa}}{3L}(2S_a - S_b - S_c) \\ \frac{di_{sb}}{dt} = -\frac{R}{L}i_{sb} - \frac{R}{L}e_b + \frac{V_{sb}}{3L}(S_a - 2S_b - S_c) \\ \frac{di_{sc}}{dt} = -\frac{R}{L}i_{sc} - \frac{R}{L}e_c + \frac{V_{sc}}{3L}(-S_a - S_b - 2S_c) \end{cases} \quad (4)$$

We applied d - q transformation and using an angular frequency of the grid line can be written as:

$$\frac{d}{dt} \begin{bmatrix} i_d \\ i_q \end{bmatrix} = \begin{bmatrix} -\frac{R}{L} & \omega \\ \omega & -\frac{R}{L} \end{bmatrix} \begin{bmatrix} i_d \\ i_q \end{bmatrix} - \begin{bmatrix} -\frac{1}{L} & 0 \\ 0 & -\frac{1}{L} \end{bmatrix} \begin{bmatrix} e_d \\ e_q \end{bmatrix} + \begin{bmatrix} V_d \\ V_q \end{bmatrix} \quad (5)$$

Where: $i_{dq} = K_{abc}^{dq} i_{abc}$, $e_{dq} = K_{abc}^{dq} e_{abc}$

The transformation matrix K_{abc}^{dq} is given as

$$K_{abc}^{dq} = \frac{2}{3} \begin{bmatrix} \cos(\theta) & \cos\left(\theta - \frac{2\pi}{3}\right) & \cos\left(\theta + \frac{2\pi}{3}\right) \\ \sin(\theta) & \sin\left(\theta - \frac{2\pi}{3}\right) & \sin\left(\theta + \frac{2\pi}{3}\right) \\ \frac{1}{2} & \frac{1}{2} & \frac{1}{2} \end{bmatrix} \quad (6)$$

The instantaneous active and reactive power which is delivered to the grid line in d - q rotating frame, $e_d = 0$. Therefore

$$\begin{cases} P = \frac{2}{3} e_d i_d \\ Q = \frac{2}{3} e_q i_d \end{cases} \quad (7)$$

The active power P can be controlled by i_q current and reactive power Q can be controlled by i_d current.

3. Design of the integral sliding mode controller

Assuming lossless power transmission between solar array and grid line, the following relationship

is obtained from (7) if reactive power is controlled zero by setting $i_d = 0$.

$$P_{pv} = P_{grid} = \frac{2}{3} e_d i_q \quad (8)$$

The proposed integral sliding surface is defined as follows:

$$\begin{cases} S(i_s) = i_d^* - i_d + C_d \int_0^t (i_d^* - i_d) dt \\ S(i_q) = i_q^* - i_q + C_q \int_0^t (i_q^* - i_q) dt \end{cases} \quad (9)$$

Where: $i_q^* = \frac{3}{2} \frac{P_{ref}}{e_d}$, and $i_d^* = 0$

P_{ref} is the reference solar array power which is given by the MPPT controller.

The control input is chosen to have the structure as follows: [7]

$$\begin{cases} V_d = V_{d-eq} + V_{d-nd} \\ V_q = V_{q-eq} + V_{q-nq} \end{cases} \quad (10)$$

Where V_{eq} is an equivalent control vector, V_{ni} is the switching part of the control (the correction factor).

The equivalent control input is obtained from the invariance condition and given by the following condition as

$$S = 0 \text{ And } \dot{S}_i = 0 \Rightarrow V_i = V_{eq} \quad (11)$$

Summarizing, the equivalent control input is given as:

$$\begin{cases} V_{d-eq} = Ri_d - \omega L_q i_q + e_d + C_d (i_d^* - i_d) \\ V_{q-eq} = Ri_q + \omega L_q i_d + e_q + C_q (i_q^* - i_q) \end{cases} \quad (12)$$

The nonlinear switching input V_{ni} can be chosen as follows:

$$V_{ni} = K \cdot \text{sgn}(S_i) \quad (13)$$

4. Mppt controller design

The sliding mode technique consists to bring the power of the load unit to the area where the power of the photovoltaic generator is operating in its maximum output.

We choice of the switching surface function by:

$$S(I_{pv}) = \frac{\partial P_{pv}}{\partial I_{pv}} = \frac{\partial I_{pv}}{\partial V_{pv}} V_{pv} + I_{pv} = 0 \quad (14)$$

$$\frac{dV_{pv}}{dt} = \frac{I_{pv}}{C} - \frac{i_L}{C} D \quad (15)$$

The equations (3) can be rewritten in the variable state form:

The control algorithm is defined by the

relation: $D = D_{eq} + D_n$

Where D_{eq} is an equivalent control vector D_{ni} is the switching part of the control (the correction factor).

The equivalent control input is obtained from the invariance condition and given by the following condition as

$$S = 0 \text{ And } \dot{S}_i = 0 \Rightarrow D_i = D_{eq} \quad (16)$$

$$D_{eq} = \frac{-\dot{i}_{pv}}{i_L} \quad (17)$$

The nonlinear switch control signal can be selected as

$$D_n = \begin{cases} 0 & S(I_{pv}) \geq 0 \\ 1 & S(I_{pv}) < 0 \end{cases} \quad (18)$$

Therefore, the ranges of the switching gains are given as follows:

$$D = \frac{-\dot{i}_{pv}}{i_L} + K_D \text{sgn}(S(I_{pv})) \quad (19)$$

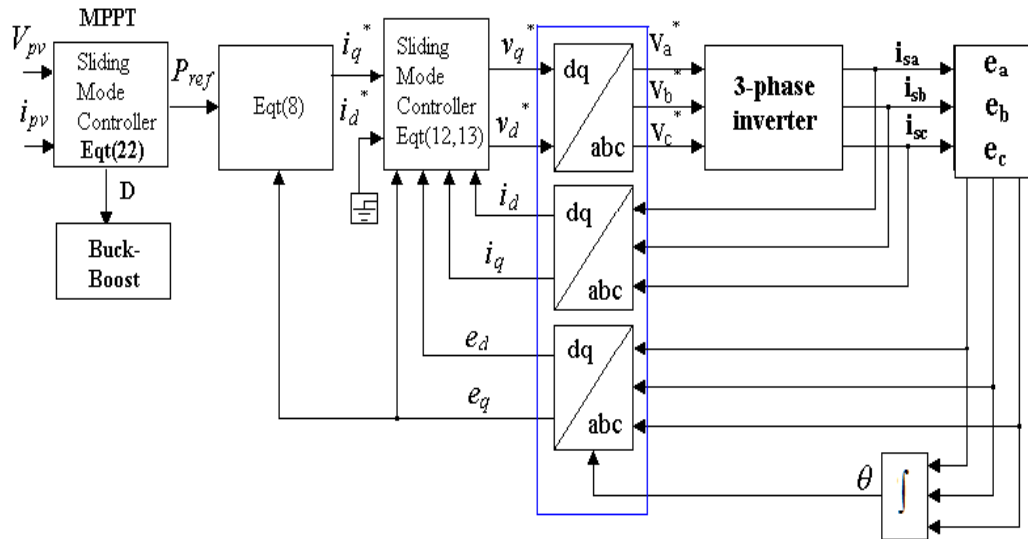


Fig.4. Detailed structure of a grid-connected PV system

5. Results of the simulation in dynamic system

In this paper, the simulation results of the sliding mode controller of power of PV grid-connected system are presented. All parameters of the photovoltaic system components are depicted in Appendix A. We applied every 0.2sec, three irradiance levels $G = 700 \text{ W/m}^2$, $G = 300 \text{ W/m}^2$ and $G = 1000 \text{ W/m}^2$ at $T = 25^\circ\text{C}$.

We can see that the appearance of the voltage and the power delivered by the PV generator are well regulated and that both variables follow their optimal references Figures.5.a, b and 5.c

The direct current i_d is in a good agreement with zero value as a command value, and then the quadratic current i_q response goes towards the optimal reference value (fig.5.d),

At the first of irradiance level of $G = 700 \text{ W/m}^2$ where the value of the maximum power delivered by GPV is 55.4 W corresponding to a optimal voltage value 17.3 V, and the quadratic current varying around the optimal reference value 1.62 A (Figure 5.a,c-5.d).

When irradiance decreases to 300 W/m^2 , there is a decrease in maximum power of GPV to 22.6

W, corresponding to an optimal voltage value of 16.63 V, and a quadratic current decreased by approximately 0.7A.

Another sudden increase of irradiation 500 W / m², gives a maximum power output of 80 W, which corresponds to the optimal voltage 17.6 V and a quadratic current optimal $i_q = 2.4$ A

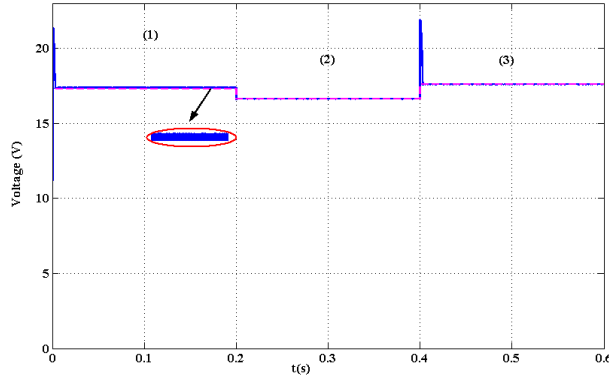


Fig.5.a. Voltage $V_{pv}(t)$, - - - $V_{pv,ref}$

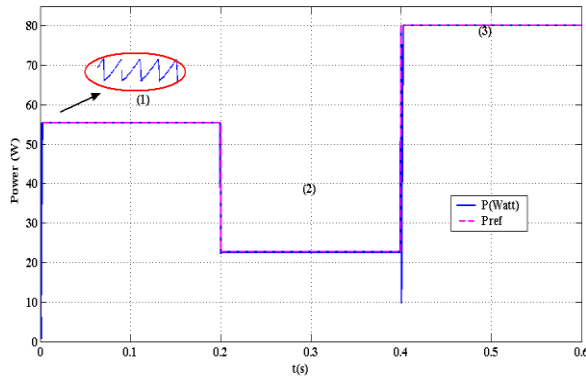


Fig.5.c. Power $P_{pv}(t)$, - - - P_{ref}

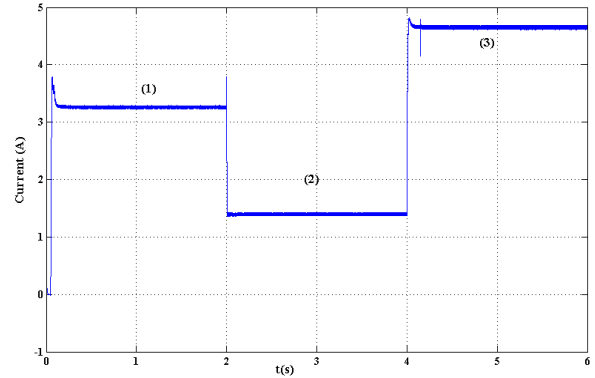


Fig.5.b. Current $I_{pv}(t)$

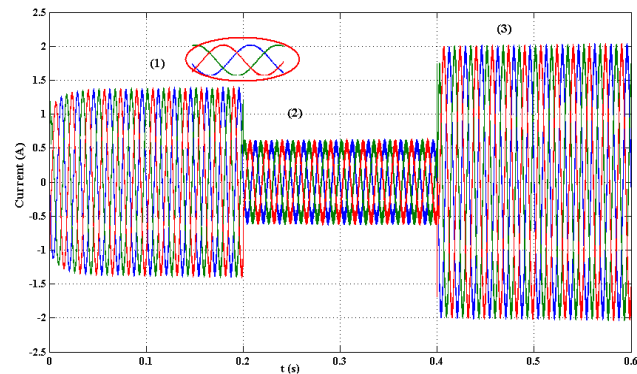
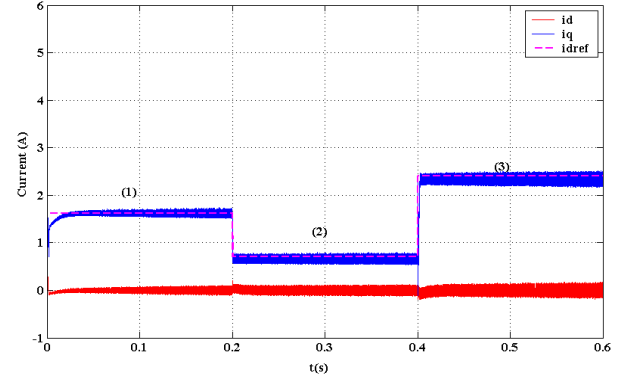


Fig.5.e. Current $i_{sa}(t)$, $i_{sb}(t)$, $i_{sc}(t)$

Fig.5. Simulation results for different sizes of grid connected photovoltaic system after optimization

$T = 25^{\circ}\text{C}$, (1) $G = 700 \text{ W/m}^2$, (2) $G = 300 \text{ W/m}^2$, (3) $G = 1000 \text{ W/m}^2$

We see a good response from the tracking system from the point of maximum power and a drawback of this technique is oscillation of (V_{pv} , I_{pv})

6. Simulation results in steady state.

The different parameters of photovoltaic system in steady state are shown in Fig.6. We used a range

of irradiance from 200 W/m² to 1000 W/m² and at two temperature 0°C and 75°C.

From the load characteristic in Fig 6.a, illustrating the operating points and the curve representing the maximum power point of the

PV array, we obtain a perfect concordance of these two curves.

The increase in temperature has a negative effect on the maximum power of PV; it illustrates the operating point of induction motor which will be supplied by voltages closer to the optimal values between 18.8V and 19.2V at a

temperature of 0°C and between 14V and 14.4V at 75°C.

After the optimization, the global power delivered by the PV array is well exploited with an error margin of about 0.09% to 0.163% for the range [200-500 W/m²] and about 0.05% to 0.08% for [500-1000 W/m²].

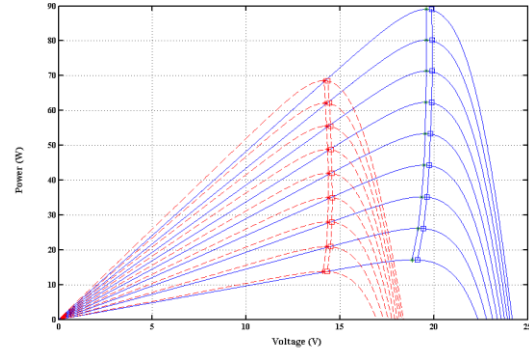
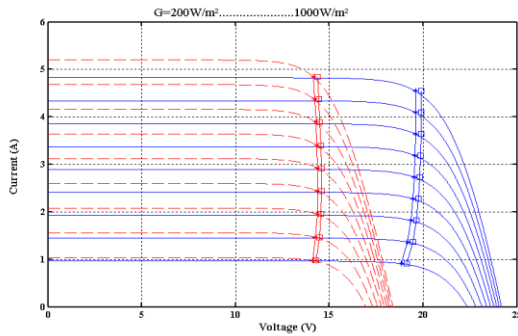


Fig.6.a. Operating point Fig.6.b. Operating point P_{pv} - V_{pv}

Fig.6. Simulation results for different sizes of the photovoltaic system

-- T = 75°C ____ T = 0 °C

7. Conclusion

In this paper, present an integral sliding mode controller of maximum power point tracking of the three-phase grid connected photovoltaic system. The main concluding remarks are summarized as follows:

- The integral sliding mode parameters for fast response, good transient performance and sensitivity to variations in external disturbances. The selecting approach of the control variables is described in figure 5a-f and figure 6a-g.
- The disadvantage of this technique is Chattering which is generally undesirable because it adds to the spectrum of command high frequency components. To overcome this drawback, a combination with techniques like fuzzy sliding mode... etc is required.
- This technique presents a simple robust control algorithm that has the advantage to be easily implantable in calculator.
- This technique presents a simple robust control algorithm that can be easily implantable in calculators.
- The disadvantage of this technique is chattering which is generally undesirable because it adds a high frequency components to the spectrum of the GPV voltage and current. To overcome this

drawback, a combination with techniques like fuzzy sliding mode should be considered... etc.

8. Annexe.

Suntech photovoltaic module 80

- $I_{sc}=4.95A$; $I_{mp}=4.85A$; $V_{oc}=21.9V$; $V_{mp}=17.5V$; $\mu_{Isc}=0.02mA/^{\circ}C$; $\mu_{voc}=-0.03mV/^{\circ}C$; $N_{cs}=36$
- Number of panels: 1 panel.
- **Parameters of grid connected [13]**
- $V=22.8V_{ep}$, $f=60Hz$, $I=4.45A$, $R_r=0.5\Omega$, $L=5mH$, $C=1000\mu f$
- $K_d=150$, $K_q=150$, $C_d=150$, $C_q=1000$, $C_v=1000$, $K_D=150$

Nomenclature

- I_{pv} generator current (A)
- I_L light current (A)
- I_o reverse saturation current (A)
- i_d d-axis stator current (A)
- i_q q-axis stator current (A)
- K Boltzmann's constant (1.08.1023J/K)
- L Inductance of DC-DC converter (H)
- L_r Self-inductance of grid (H)
- q electronic charge (1.9.10⁻¹⁹ C)
- R_s equivalent series resistance of PV (Ω)

R_r stator resistance of grid per phase (Ω)
 V_{pv} output generator voltage (V)
 V_d d-axis grid voltage (V)
 V_q q-axis grid voltage (V)
 ω_s synchronous angular speed (rd/s)
 E_g voltage band gap (1.12eV)
 D duty cycle
 G irradiation (W/m^2)
 μ_{Isc} temperature coefficient of I_{sc} ($A/^{\circ}C$)
 μ_{osc} temperature coefficient of V_{oc} ($V/^{\circ}C$)

References:

1. A. Kotsopoulos et al. A predictive control scheme for DC voltage and AC current in grid-connected photovoltaic inverters with minimum dc link capacitance, IECON, 1994–1969, 2001.
2. Alghuwainem, SM. Application of a DC chopper to maximize utilization of solar-cell generators. pp. 91 WM, 145-3 EC, 1991 IEEE/PES 1991 winter meeting, New York, 3–7 February 1991.
3. A. Yazdani, P.P. Dash. A Control Methodology and Characterization of Dynamics for a Photovoltaic (PV) System Interfaced With a Distribution Network. IEEE Trans. Power Del., vol. 24, no. 3, pp. 1538–1551, Jan. 2009.
4. C. Hua, J. Lin. An On-Line MPPT Algorithm for Rapidly Changing Illuminations of Solar Arrays. Renewable Energy, Vol. 28, N°7, pp. 1129 - 1142, 2003.
5. F. Valenciana, P.F. Puleston, P.E. Battaiotto. Power control of a photovoltaic array in a hybrid electric system using sliding mode techniques. Proc. Inst. Elect. Eng., Contr. Theory Appl., vol. 148, no. 6, pp. 448–455, Nov. 2001.
6. Hussein K H, Muta I, Hoshimo T, Oskada M. Maximum photovoltaic power tracking an algorithm for rapidly changing atmospheric conditions, generation, transmission and distribution. IEE Proceedings, vol. 142, no. 1, pp. 59-64, 1995.
7. Il. Song Kim. Sliding mode controller for the single-phase grid-connected photovoltaic system. Applied Energy 83 (2006) 1101–1115.
8. R. Chenni, M. Makhlouf, T. Kerbach, A. Bouzid. A detailed modeling method for photovoltaic cells. Energy; 2007, vol 32, 1724–1730.
9. R.D. Biel and Enric Fossas et al., Application of sliding-mode control to the design of a buck-based sinusoidal generator, IEEE Trans Industrial Electronics Vol. 48, No. 3, 563–571, 2001.
10. S. Lalouni, D. Rekioua, T. Rekioua, E. Matagne. Fuzzy logic control of stand-alone photovoltaic system with battery storage, Journal of Power Sources, September 2009, Volume 193, Issue 2, pp. 899-907.
11. Sh. Morimoto. Sensorless Output Maximization Control for Variable-Speed Wind Generation System Using IPMSG. IEEE Transactions on industry applications, Vol. 41, N°. 1, January/February 2005.
12. V. Salas, E. Olías, A. Barrado, Review of the Maximum Power Point Tracking Algorithms for Stand-Alone Photovoltaic Systems. Solar Energy Materials & Solar Cells, 2006, vol 90, N°: 11, pp: 1555 –1578.
13. Valenciana F, Puleston PF, Battaiotto PE. Power control of a photovoltaic array in a hybrid electric generation system using sliding mode techniques. IEE Proc-Control Theory Appl 2001; 148(6):P448–55.
14. Il. Song Kim. Sliding mode controller for the single-phase grid-connected photovoltaic system. Applied Energy 83 (2006) 1101–1115.